



Cite this: *Lab Chip*, 2019, 19, 1977

On-the-fly exchangeable microfluidic nozzles for facile production of various monodisperse micromaterials†

Tom Kamperman, ‡*, Bas van Loo, ‡, Melvin Gurian,  Sieger Henke, Marcel Karperien  and Jeroen Leijten *

Microfluidic manufacturing platforms have advanced the production of monodisperse, shape-controlled, and chemically defined micromaterials. However, conventional microfabrication platforms are typically designed and fabricated as single-purpose and single-use tools, which limits their efficiency, versatility, and overall potential. We here present an on-the-fly exchangeable nozzle concept that operates in a transparent, 3D, and reusable microfluidic device produced without cleanroom technology. The facile exchange and repositioning of the nozzles readily enables the production of monodisperse water-in-oil and oil-in-water emulsions, solid and core-shell microspheres, microfibers, and even Janus type micromaterials with controlled diameters ranging from 10 to 1000 μm using a single microfluidic device.

Received 16th January 2019,
Accepted 13th April 2019

DOI: 10.1039/c9lc00054b

rsc.li/loc

Introduction

Microfluidic devices offer predictable (*i.e.*, laminar) flow behaviour, in-line manipulation, and monitoring of liquids.¹ This control over liquids has enabled the production of micromaterials with controlled size, shape, and composition.^{2–4} Microfluidic devices are typically produced as channels that are permanently formed and/or enclosed within glass or transparent polymer using a covalent bonding strategy such as plasma bonding, gluing, or fusing *via* partial melting or dissolving.^{5,6} The non-reversible nature of these conventional microfluidic device fabrication methods limits their use to a single specific application. In particular, device dimensions and surface wetting properties need to be optimized per application, with little to no flexibility for efficient adaptation to other applications.^{7,8} Conventional microfluidic devices are also inefficient during design optimization strategies, as their non-adaptable nature hampers swift iterations towards a functional device. On top, conventional micro-devices are considered as single-use disposables. Cleaning difficulties of permanently bonded devices contributes to significant wastage of (*e.g.*, clogged) chips, which is highly cost-inefficient considering the high-end materials, skilled personnel, and advanced lithographic infrastructure that are typi-

cally required for manufacturing of microfluidic devices. These limitations have jointly been hampering the rapid and widespread adoption of microfluidic technologies into other scientific disciplines as well as translation into clinical and industrial applications.^{9,10}

Opportunely, microfluidic devices with on-demand adaptable channels represent a straightforward flexible solution to expand the versatility and efficiency of microfluidic devices. Reusable ‘off-the-shelf’ microfluidic devices made from plastic parts and steel needles have been explored to this end. These devices have been successfully used for flow focusing applications,¹¹ generation and splitting of water-in-oil (W/O) droplets,^{12,13} and liposome generation.¹⁴ However, the non-transparent nature of current devices impaired the direct monitoring that is required for controlled droplet formation and manipulation processes. Nozzle positioning has, for example, a major effect on the droplet size.¹⁵ Furthermore, microfluidic device transparency is critical for the on-chip photocrosslinking of various polymers.¹⁶ The pressing need for on-the-fly adaptable microfluidic devices is furthermore reflected by the recent development of several modular microfluidic systems.^{17–20} Regardless of their promise, current adaptable microfluidic devices are not yet readily compatible with the production of solid micromaterials.

In this work, we demonstrate the fabrication of monodisperse micrometer-sized droplets, beads, and fibers using a fully transparent multifunctional 3D microfluidic device with exchangeable nozzles. The microfluidic device was manufactured without cleanroom technology and could be configured on-the-fly to operate in a T-junction, coaxial flow, and flow focusing manner. Combining this multifunctional

Department of Developmental BioEngineering, Faculty of Science and Technology, Technical Medical Centre, University of Twente, Drienerloolaan 5, 7522 NB Enschede, The Netherlands. E-mail: t.kamperman@utwente.nl, jeroen.leijten@utwente.nl

† Electronic supplementary information (ESI) available: Experimental section, Fig. S1–S5, Movie S1. See DOI: 10.1039/c9lc00054b

‡ Co-first authors/contributed equally to this work.



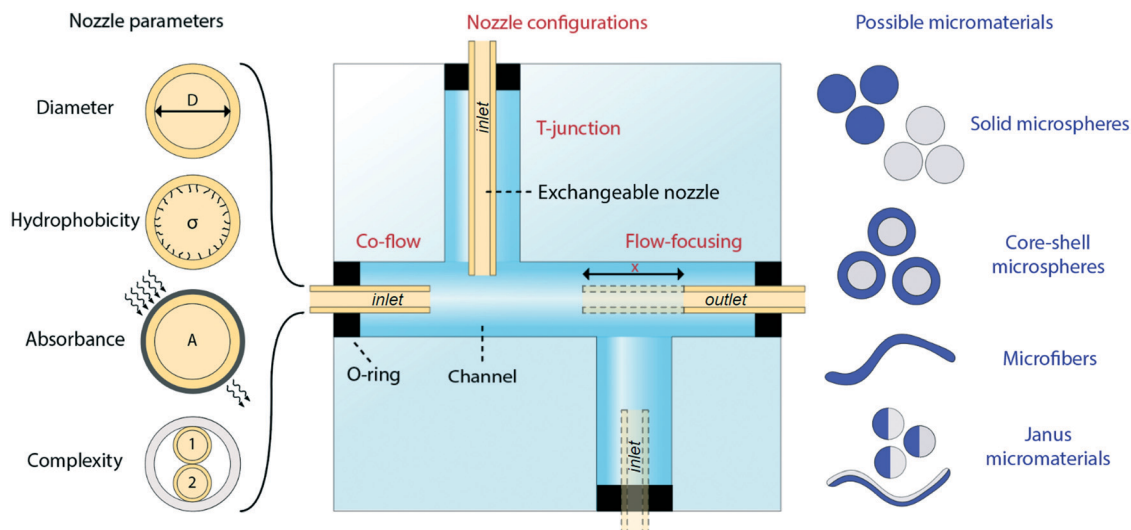


Fig. 1 Schematic concept of exchangeable nozzles within a multifunctional 3D microfluidic device for versatile monodisperse micromaterials production. Sealed connections between the device, tubing, and nozzles enable the on-the-fly exchange of nozzles. This allows for the on-demand switching between nozzles with different diameters, hydrophobicity, absorbance, and complexity. Furthermore, the nozzle placement can be temporally controlled to switch between T-junction, co-flow, and flow-focusing configurations. The multifunctional nature of this microfluidic device enables facile tuning towards the fabrication of emulsions and various micromaterials including microspheres and microfibers.

microfluidic production platform with various classes of *in situ* crosslinkable polymers enabled the straightforward

micromanufacturing of myriad micromaterials with controlled size, shape, composition, and complexity (Fig. 1).

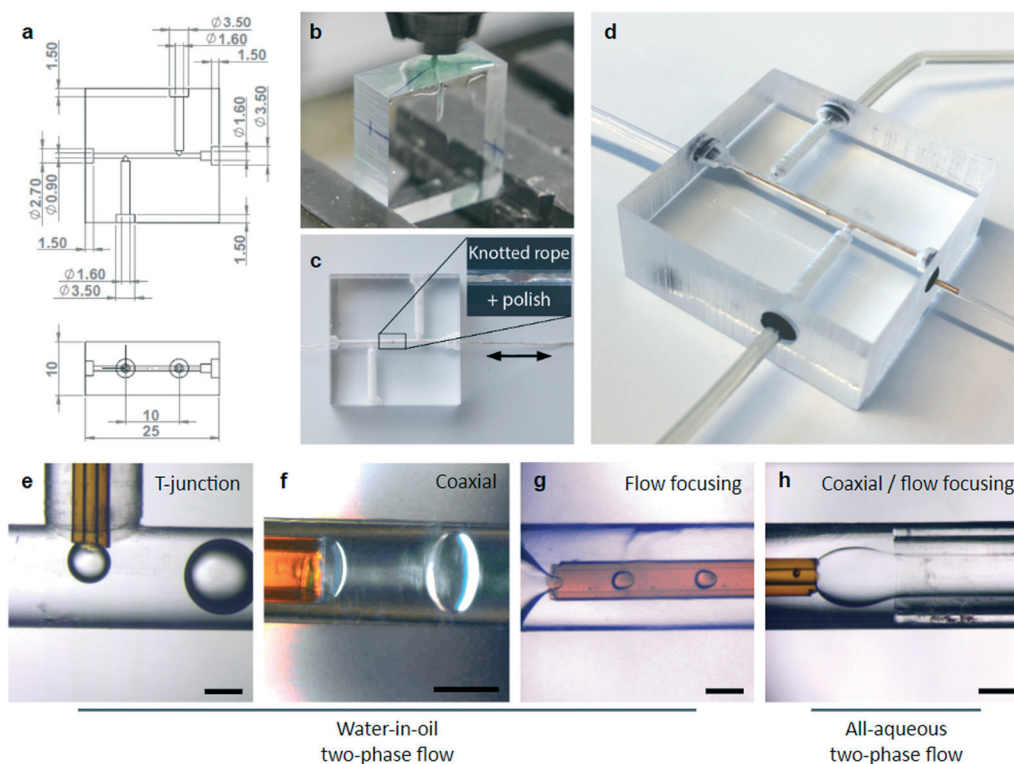


Fig. 2 Engineering a microfluidic device with exchangeable nozzles. (a) Computer-aided design (CAD) of the multifunctional 3D microfluidic device. The device was fabricated in PMMA using standard (b) cutting (i.e., sawing and micromilling) and (c) abrasion (i.e., polishing) techniques. (d) Tubing and nozzles were sealed to the PMMA device using rubber O-rings that auto-centered inserted nozzles. The adaptable nature of the microfluidic device enabled the straightforward generation of water-in-oil and all-aqueous two-phase flows using (e) T-junction, (f) coaxial, (g) flow focusing, and (h) coaxial/flow focusing nozzle configurations. Scale bars indicate 350 μm .



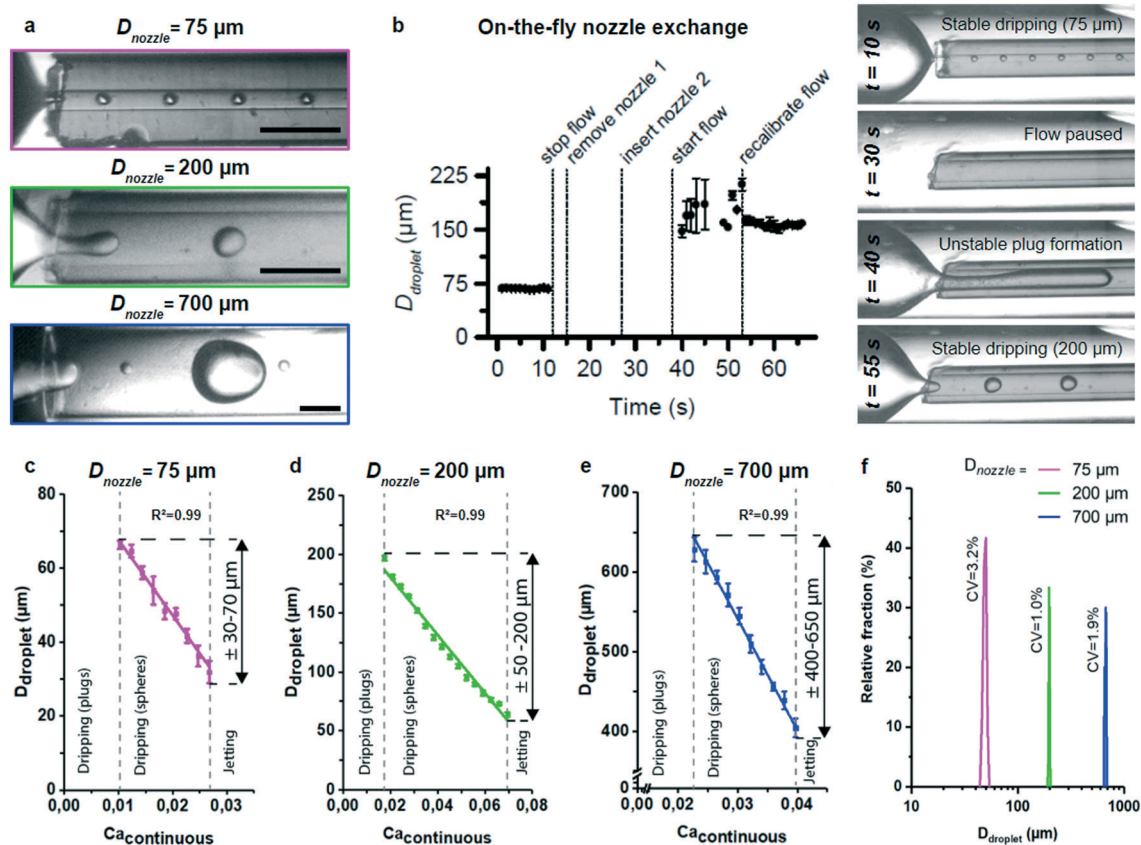


Fig. 3 Characterization of microdroplets production with on-the-fly nozzle exchange. (a) Coaxially flowing water in oil using nozzles with different inner diameters enabled the formation of droplets with diameters spanning more than an order of magnitude. (b) Switching between two stable droplet production size regimes by exchanging the nozzle was achieved within one minute. (c–e) Per nozzle, the droplet size was fine-tuned by tuning the flow rate of the continuous phase and thereby the capillary number. (f) All nozzles were compatible with the production of monodisperse ($CV < 5\%$) droplets. Scale bars indicate 350 μm .

Results and discussion

Design and fabrication of multifunctional microfluidic device with exchangeable nozzles

The microfluidic device design consisted of a center channel and two side channels that essentially formed two serially connected T-junctions (Fig. 2a). This design was compatible with the user-defined assembly of a variety of nozzles into the three most used nozzle configurations, namely T-junction, coaxial flow, and flow focusing, and thus acted as a universal platform for the fabrication of a variety of micromaterials.

The device was fabricated in polymethylmethacrylate (PMMA), as this material is transparent, widely available, and biocompatible, but also mechanically robust while easily adaptable using standard cutting and abrasion methods. Channels were micromilled in the presence of concentrated soap solution that acted as a coolant and prevented heat-induced cracking of the PMMA, resulting in precise and highly reproducible microfluidic device fabrication (Fig. 2b).²¹ Channels were measured to be 0.9 mm in diameter, which allowed for the insertion of a wide variety of commercially available capillaries. The device inlets and outlets consisted of

1.6 mm wide holes that enabled the insertion of 1/16" (*i.e.*, $\sim 1.59 \text{ mm}$) outer diameter tubing, which is commonly used in microfluidic applications. After micromilling, the transparency of the center channel was increased by >2.5 -fold through abrasion using a knotted thread and polish (Fig. 2c and S1†).

Fused silica capillaries were selected as nozzles, as they are readily available with inner diameters ranging from 2 ± 1 to $700 \pm 10 \mu\text{m}$ and outer diameters ranging from 90 ± 6 to $850 \pm 20 \mu\text{m}$, thus nearly spanning the entire micrometer regime. Furthermore, fused silica capillaries can be pre-coated with, for example, a polyimide layer to improve durability and provide UV-protection. Exchangeable nozzles were fabricated by gluing a fused silica capillary into 1/16" tubing (*i.e.*, for T-junction and coaxial flow) or by inserting it into silicone tubing (*i.e.*, for flow focusing), which acted as outlet tubing (Fig. S2†). The transparent and semi-permeable nature of the silicone outlet tubing enabled in-line monitoring, photo-irradiation of the flowing materials, and diffusion-based delivery of small molecules such as reactive hydrogen peroxide to induce or control chemical reactions.²²

The microfluidic device inlets and outlets were partially widened to hold elastic O-rings that formed liquid tight seals and ensured centring of the exchangeable nozzles and/or



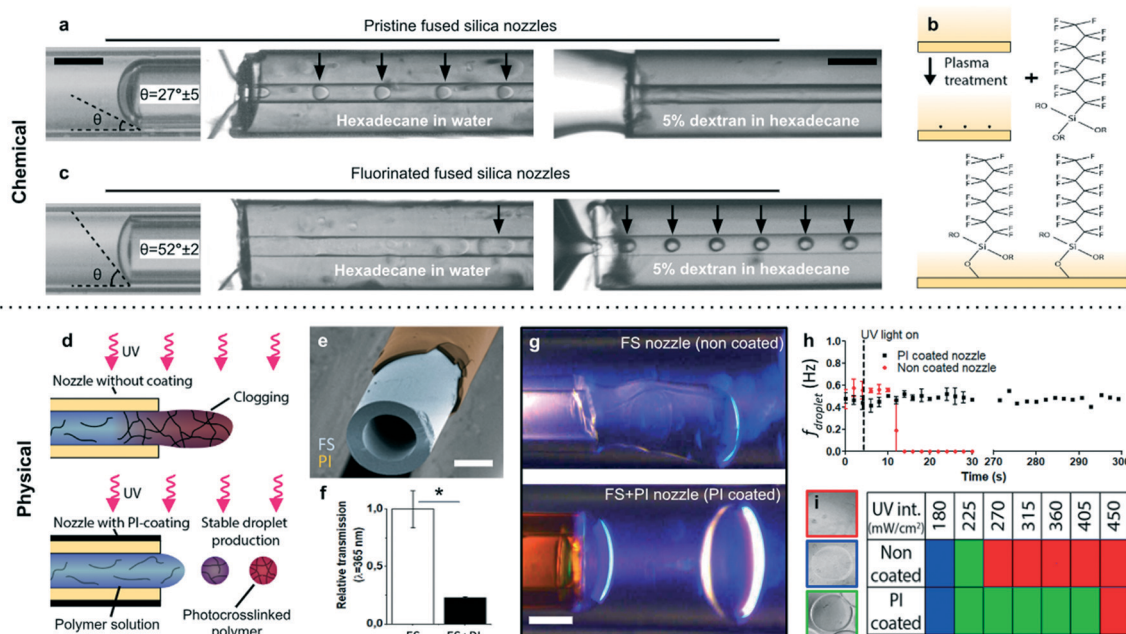


Fig. 4 Chemical and physical optimization of exchangeable nozzles to enable the processing of polymers solutions. (a) Pristine fused silica nozzles were hydrophilic, which readily enabled the formation of O/W emulsions, but impaired the formation of polymer-laden W/O emulsions such as dextran solution in hexadecane. (b) Chemically treating the fused silica with fluorinated silane (c) resulted in less hydrophilic nozzles that were compatible with the production of polymer-laden W/O emulsions. (d and e) Alternatively, fused silica (FS) nozzles could be physically modified with a UV-protective polyimide (PI) coating to prevent nozzle clogging during processing of photocrosslinkable polymers. (f) The polyimide coating reduced the relative UV transmission by more than 4-fold and enabled (g and h) continuous and stable production of photocrosslinked polymer microspheres under UV irradiation by preventing nozzle clogging (i) over a wide range of UV intensities as compared to non-coated nozzles. Nozzle clogging, incomplete PEGDA photocrosslinking, and complete PEGDA photocrosslinking are indicated with red, blue, and green squares, respectively. Scale bars indicate 200 μm . * indicates significance with $p < 0.01$.

tubing in the microfluidic device's channels. Optionally, a borosilicate glass capillary spacer was used to enable sealing of the silicone tubing into the device. As expected, the PMMA device and rubber O-rings enabled the facile connection of tubing and fused silica nozzles in various configurations, as confirmed by successful demonstration of W/O emulsification using T-junction, coaxial, and flow focusing modes, as well as the formation of a focused aqueous two-phase coaxial flow (Fig. 2d–h).

Expanding the microfluidic droplet production regime using exchangeable nozzles

Microfluidic droplets can be leveraged as templates for the controlled fabrication of microspheres.²³ The size of such microfluidic-generated materials strongly depends on the nozzle width, the flow ratio of the dispersed and continuous phases, and (for droplet and particles) the capillary number of the continuous phase $Ca = \eta_c v_c / \gamma$, where η_c is the viscosity of the continuous phase, v_c is the average velocity of the continuous phase, and γ is the interfacial tension between the dispersed and continuous phases.²⁴ Tuning the flow rates of the dispersed and continuous phases is thus a potent strategy to control the droplet size. However, stable production of monodisperse droplets is limited to the squeezing and dripping regimes.^{25,26} Therefore, droplet size can only be fine-

tuned within a relatively small regime, typically limited to an order of magnitude in diameter.^{27–29} We hypothesized that the production regime of a single microfluidic device could be significantly expanded in terms of droplet size by controlling the nozzle diameter on-the-fly. To demonstrate this, our microfluidic device was successively equipped with three different nozzles ($D_{\text{nozzle}} = 75, 200, 700 \mu\text{m}$) during a continuous experiment. On-the-fly exchange of the nozzles readily enabled the production of monodisperse microdroplets with diameters exceeding an order of magnitude, as demonstrated by emulsification of water in a 1% Span 80 containing hexadecane solution (Fig. 3a). The rubber O-rings enabled facile and swift nozzle exchange by guaranteeing instant sealing and auto-centring of the nozzles, which allowed for the switching between different droplet size production regimes in less than a minute (Fig. 3b, Movie S1†). As expected, with every nozzle the droplet size could be fine-tuned by controlling the capillary number. Specifically, increasing the capillary number by increasing the continuous phase flow rate resulted in reduction of the droplet size (Fig. 3c–e). Furthermore, the exact position of nozzles significantly affected the droplet production regime, which could be uniquely simultaneously fine-tuned and monitored through on-the-fly repositioning of the nozzles within our transparent microfluidic device (Fig. S3†). Microdroplets over the entire size regime were characterized by a monodisperse size distribution



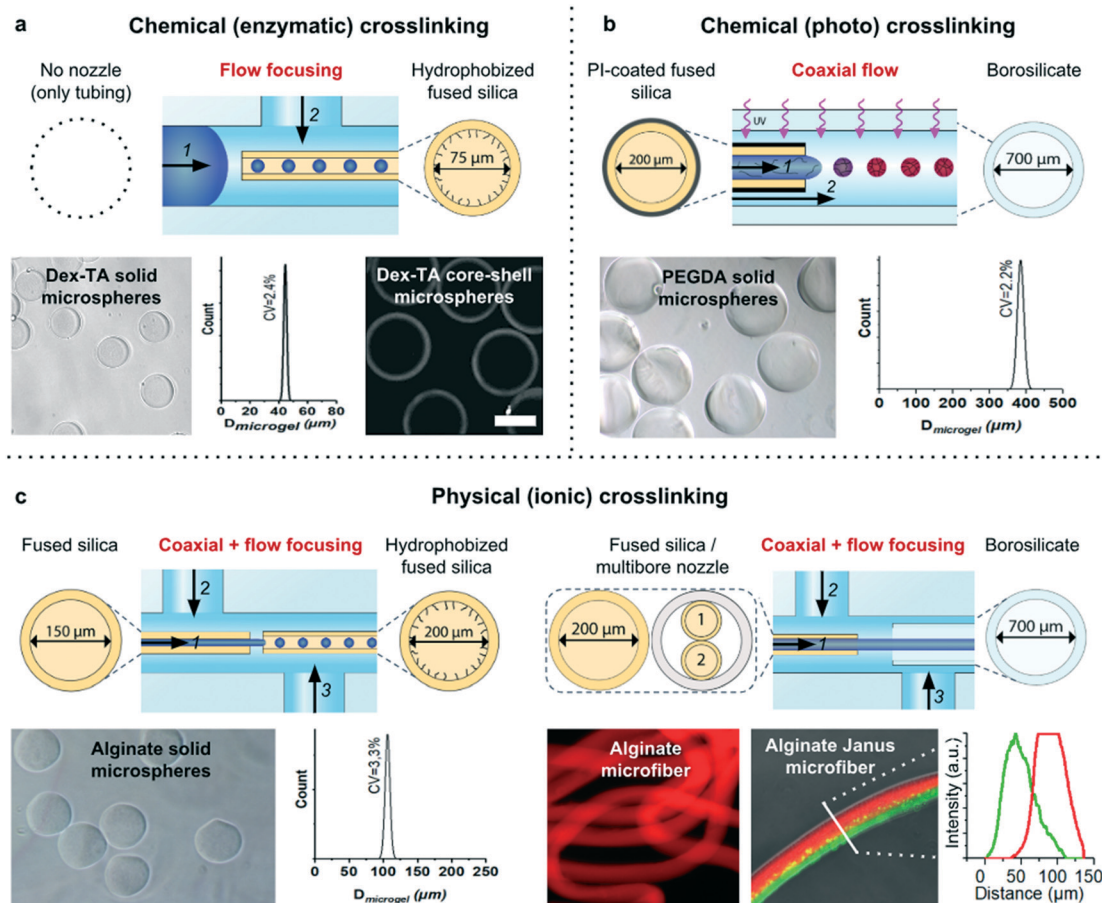


Fig. 5 Various examples of monodisperse micromaterials produced using the multifunctional 3D microfluidic device with different optimized nozzle configurations. (a) Flow focusing an enzymatically crosslinkable Dex-TA and HRP containing solution (1) in hexadecane with Span 80 (2) using a fluorinated fused silica nozzle enabled the production of monodisperse solid dextran-based microspheres. (b) Coaxially flowing a photo-crosslinkable PEGDA and I2959 containing solution (1) in hexadecane with Span 80 (2) using a polyimide-coated fused silica nozzle enabled the production of monodisperse PEG-based microspheres. (c) Focusing coaxially flowing alginate (1) and PEG (2) containing solutions in a calcium chloride containing solution (3) using a combination of single and multibore capillaries enabled the production of monodisperse simple and Janus type microfibers. Scale bar indicates 200 μm .

as confirmed by coefficients of variation $CV < 5\%$. (Fig. 3f). Similar size control was achieved with all-aqueous two-phase co-flows, which is key for the microfabrication of, for example, microfibers with controlled diameters (Fig. S4†).

Chemical and physical nozzle tuning for micromaterial production

Controlling microfluidic nozzle wettability is key to achieve successful generation of droplets. The fused silica nozzles used in this work contain siloxane bridges that bind water *via* chemisorption to form silanol groups, which adsorb polar compounds including water molecules allowing it to act as a hydrophilic surface.³⁰ Consequently, fused silica is inherently hydrophilic in its native state, which was confirmed by contact angle measurements ($\theta = 27 \pm 5^\circ$) using the capillary rise method (Fig. 4a).³¹ Fused silica nozzles were therefore readily compatible with production of oil-in-water (O/W) emulsions such as hexadecane in a 1% sodium

dodecyl sulphate (SDS) containing water solution. However, the nozzles' hydrophilic nature also hampered the stable formation of W/O emulsions. Moreover, aqueous wetting of fused silica was exacerbated in the presence of water-soluble polymers such as dextran, which hindered the formation of microsphere precursor droplets (Fig. 4a). To enable polymer microsphere formation through microfluidic emulsion templating using our microfluidic platform, fused silica nozzles were deactivated by chemically coupling fluorinated silane to the available silanol groups (Fig. 4b). The fluorinated fused silica nozzles were significantly less hydrophilic ($\theta = 52 \pm 2^\circ$) than pristine fused silica nozzles and were proven to be compatible with the W/O emulsification of 5% dextran solution (Fig. 4c).

Besides chemical modification, exchangeable nozzles could also be physically optimized for the processing of polymer precursor solutions. For example, selectively modifying the optical properties of nozzles offers the possibility to optimize the microfluidic system for processing



photocrosslinkable polymers. An ongoing challenge in on-chip photocrosslinking strategies is microfluidic channel clogging due to photocrosslinking of polymers by strayed UV light.^{32–34} To overcome UV-induced clogging, we exchanged the conventionally used glass or borosilicate capillaries by polyimide-coated fused silica capillaries that acted as UV-protected nozzles (Fig. 4d and e). Absorption spectrometry confirmed that polyimide-coated nozzles absorbed significantly more UV light ($\lambda = 365$ nm) than pristine fused silica nozzles (Fig. 4f). Advantageously, the polyimide-coated nozzles enabled the continuous and stable on-chip production of polyethylene glycol diacrylate (PEGDA) microdroplets in the presence of UV light, while the pristine nozzle mainly associated with clogging (Fig. 4g and h). Moreover, the use of polyimide-coated nozzles significantly widened the operational window for the production of completely photocrosslinked PEGDA microspheres (Fig. 4i).

On-demand fabrication of a wide variety of micromaterials

To demonstrate the universal nature of the microfluidic device, it was combined with a variety of nozzles in different configurations to produce various different classes of micromaterials. To this end, several combinations of distinct (i) polymers (natural and synthetic); (ii) crosslinking mechanisms (chemical and physical); (iii) morphologies (spherical and fiber); and (iv) complexities (isotropic solid, Janus solid, and core-shell) were produced (Fig. 5).

A flow focusing configuration of a fluorinated fused silica nozzle enabled the stable production of isotropic solid and core-shell dextran microspheres (Fig. 5a). Specifically, a mixture of dextran-tyramine (Dex-TA) and horseradish peroxidase (HRP) was emulsified with hexadecane that contained Span 80, and flown through a semi-permeable silicone tubing that was submerged in H_2O_2 . Diffusion-based supplementation of H_2O_2 into the polymer droplets initiated the enzymatic crosslinking of the tyramine moieties resulting in the formation of monodisperse dextran microspheres.²² Core-shell microspheres were produced by adding the H_2O_2 consuming enzyme catalase to the polymer solution,^{35,36} which prevented crosslinking of the droplet center.

A polyimide-coated capillary in coaxial flow mode was used as a UV-shielded nozzle to demonstrate the stable production of photocrosslinked PEGDA microspheres (Fig. 5b). Acrylate moieties of PEGDA can be covalently coupled through free-radical polymerization upon irradiation of a photoinitiator such as 2-hydroxy-4'-(2-hydroxyethoxy)-2-methylpropiophenone (I2959). Straightforward W/O emulsification of a PEGDA and I2959 containing solution using a UV-irradiated coaxial flow nozzle resulted in the stable and clog-free formation of monodisperse PEGDA microspheres. A combination of coaxial flow and flow focusing was used to generate alginate microspheres (Fig. 5c). Specifically, this nozzle arrangement enabled the formation of a laminar three-layered co-flow of CaCO_3 nanoparticles in alginate, Span 80

in hexadecane, and Span 80 and acetic acid in hexadecane. The alginate droplets were ionically crosslinked using divalent calcium cations, which were released upon the acid-induced dissolution of CaCO_3 .³⁷ The middle oil flow acted as a liquid barrier between the CaCO_3 and the acetic acid, which prevented clogging of the microfluidic device. Alginate microfibers were produced using the same nozzle configuration by coflowing solutions of alginate, polyethylene glycol (PEG) and CaCl_2 . The middle PEG flow acted as a liquid barrier between the divalent calcium ions and the alginate, which prevented microfluidic device clogging. Inserting a multibore nozzle readily provided an extra level of complexity, as demonstrated by the production of Janus type microfibers (Fig. 5c and S5†).

Conclusions

Microfluidic platforms for micromaterial production typically rely on permanently enclosed single-use devices with limited operational freedom. In this work, we presented a re-usable microfluidic device with disposable exchangeable nozzles, which enabled the controlled production of a wide variety of micromaterials. The device was fabricated in PMMA using standard cutting and abrasion methods that do not demand clean-room infrastructures. Reversible exchange of the tubing, nozzles, and device was enabled in a rapid, straightforward, and leak-free manner. On-the-fly nozzle exchange enabled the continuous generation of microfluidic products over a size range far exceeding the production limits of conventional fixed nozzle devices. Furthermore, nozzle exchange readily allowed for the tuning of surface wetting properties, which enabled swift iteration towards functional micro-manufacturing protocols for various materials. Various nozzle configurations, materials, and crosslinking methods have been efficiently and successfully combined to demonstrate the user-friendly manufacturing of a myriad of micromaterials. Uniquely, equipping the transparent microfluidic device with UV-protected nozzles enabled the stable production of photocrosslinked polymer microspheres. The universal and facile nature of the transparent 3D microfluidic device with exchangeable nozzles is expected to facilitate the controlled production of micromaterials, thereby aiding its widespread adoption.

Conflicts of interest

There are no conflicts of interest to declare.

Acknowledgements

The authors acknowledge prof. P. J. Dijkstra for his help with Dex-TA synthesis. MK acknowledges financial support from the Dutch Arthritis Foundation (#LLP-25). JL acknowledges financial support from an Innovative Research Incentives Scheme Veni award (#14328) from the Netherlands Organization for Scientific Research (NWO), the European Research Council (ERC, Starting Grant, #759425), and the



Dutch Arthritis Foundation (#17-1-405). Conception by TK, SH, and JL. JL also acknowledge funding from the National Institutes of Health (R01AR074234). Experimental design by TK, BvL, and JL. Experiments performed by TK, BvL, and MG. Data interpretation by all authors. Manuscript written by TK and JL. Supervision and revisions by TK, MK, and JL.

References

- 1 G. M. Whitesides, The origins and the future of microfluidics, *Nature*, 2006, **442**(7101), 368–373.
- 2 S. Ma, *et al.*, Fabrication of microgel particles with complex shape via selective polymerization of aqueous two-phase systems, *Small*, 2012, **8**(15), 2356–2360.
- 3 E. Kang, *et al.*, Digitally tunable physicochemical coding of material composition and topography in continuous microfibrils, *Nat. Mater.*, 2011, **10**(11), 877–883.
- 4 S. Xu, *et al.*, Generation of monodisperse particles by using microfluidics: control over size, shape, and composition, *Angew. Chem., Int. Ed.*, 2005, **44**(5), 724–728.
- 5 Y. Temiz, *et al.*, Lab-on-a-chip devices: How to close and plug the lab?, *Microelectron. Eng.*, 2015, **132**, 156–175.
- 6 G. S. Fiorini and D. T. Chiu, Disposable microfluidic devices: fabrication, function, and application, *BioTechniques*, 2005, **38**(3), 429–446.
- 7 W. A. Bauer, *et al.*, Hydrophilic PDMS microchannels for high-throughput formation of oil-in-water microdroplets and water-in-oil-in-water double emulsions, *Lab Chip*, 2010, **10**(14), 1814–1819.
- 8 S. L. Anna, Droplets and Bubbles in Microfluidic Devices, *Annu. Rev. Fluid Mech.*, 2016, **48**(1), 285–309.
- 9 C. Holtze, Large-scale droplet production in microfluidic devices—an industrial perspective, *J. Phys. D: Appl. Phys.*, 2013, **46**(11), 114008.
- 10 C. Holtze, A. S. Weisse and M. Vranceanu, Commercial Value and Challenges of Drop-Based Microfluidic Screening Platforms—An Opinion, *Micromachines*, 2017, **8**(6), 193.
- 11 A. Terray and S. J. Hart, “Off-the-shelf” 3-D microfluidic nozzle, *Lab Chip*, 2010, **10**(13), 1729–1731.
- 12 T. Li, *et al.*, Simple and reusable off-the-shelf microfluidic devices for the versatile generation of droplets, *Lab Chip*, 2016, **16**(24), 4718–4724.
- 13 Y. Wang, *et al.*, Controllable geometry-mediated droplet fission using “off-the-shelf” capillary microfluidics device, *RSC Adv.*, 2014, **4**(59), 31184–31187.
- 14 E. Bottaro and C. Nastruzzi, “Off-the-shelf” microfluidic devices for the production of liposomes for drug delivery, *Mater. Sci. Eng., C*, 2016, **64**, 29–33.
- 15 K. Wang, *et al.*, Generation of micromonodispersed droplets and bubbles in the capillary embedded T-junction microfluidic devices, *AIChE J.*, 2011, **57**(2), 299–306.
- 16 T. Kamperman, *et al.*, Single Cell Microgel Based Modular Bioinks for Uncoupled Cellular Micro- and Macroenvironments, *Adv. Healthcare Mater.*, 2017, **6**(3), 1600913.
- 17 S. Dekker, *et al.*, Standardized and modular microfluidic platform for fast Lab on Chip system development, *Sens. Actuators, B*, 2018, **272**, 468–478.
- 18 V. Kevin and L. Abraham Phillip, A truly Lego®-like modular microfluidics platform, *J. Micromech. Microeng.*, 2017, **27**(3), 035004.
- 19 C. E. Owens and A. J. Hart, High-precision modular microfluidics by micromilling of interlocking injection-molded blocks, *Lab Chip*, 2018, **18**(6), 890–901.
- 20 K. C. Bhargava, B. Thompson and N. Malmstadt, Discrete elements for 3D microfluidics, *Proc. Natl. Acad. Sci. U. S. A.*, 2014, **111**(42), 15013–15018.
- 21 D. J. Guckenberger, *et al.*, Micromilling: a method for ultra-rapid prototyping of plastic microfluidic devices, *Lab Chip*, 2015, **15**(11), 2364–2378.
- 22 T. Kamperman, *et al.*, Centering Single Cells in Microgels via Delayed Crosslinking Supports Long-Term 3D Culture by Preventing Cell Escape, *Small*, 2017, **13**(22), 1603711.
- 23 J. I. Park, *et al.*, Microfluidic Synthesis of Polymer and Inorganic Particulate Materials, *Annu. Rev. Mater. Res.*, 2010, **40**(1), 415–443.
- 24 G. F. Christopher, *et al.*, Experimental observations of the squeezing-to-dripping transition in T-shaped microfluidic junctions, *Phys. Rev. E: Stat., Nonlinear, Soft Matter Phys.*, 2008, **78**(3), 036317.
- 25 J. K. Nunes, *et al.*, Dripping and jetting in microfluidic multiphase flows applied to particle and fiber synthesis, *J. Phys. D: Appl. Phys.*, 2013, **46**(11), 114002.
- 26 M. Zagnoni, J. Anderson and J. M. Cooper, Hysteresis in multiphase microfluidics at a T-junction, *Langmuir*, 2010, **26**(12), 9416–9422.
- 27 L. Yobas, *et al.*, High-performance flow-focusing geometry for spontaneous generation of monodispersed droplets, *Lab Chip*, 2006, **6**(8), 1073–1079.
- 28 S. L. Anna, N. Bontoux and H. A. Stone, Formation of dispersions using “flow focusing” in microchannels, *Appl. Phys. Lett.*, 2003, **82**(3), 364–366.
- 29 J. Wacker, V. K. Parashar and M. A. M. Gijs, Influence of Oil Type and Viscosity on Droplet Size in a Flow Focusing Microfluidic Device, *Procedia Chem.*, 2009, **1**(1), 1083–1086.
- 30 E. Papirer, *Adsorption on silica surfaces*, Marcel Dekker, Inc., 2000.
- 31 M. W. Ogden and H. M. McNair, Characterization of fused-silica capillary tubing by contact angle measurements, *J. Chromatogr. A*, 1986, **354**, 7–18.
- 32 S. Seiffert, *et al.*, Reduced UV light scattering in PDMS microfluidic devices, *Lab Chip*, 2011, **11**(5), 966–968.
- 33 S. Wang, *et al.*, An in-situ photocrosslinking microfluidic technique to generate non-spherical, cytocompatible, degradable, monodisperse alginate microgels for chondrocyte encapsulation, *Biomicrofluidics*, 2018, **12**(1), 014106.
- 34 S. Wang, *et al.*, A Very Low-Cost, Labor-Efficient, and Simple Method to Block Scattered Ultraviolet Light in PDMS Microfluidic Devices by Inserting Aluminum Foil Strips, *J. Therm. Sci. Eng. Appl.*, 2018, **11**(1), 014501.



- 35 T. Kamperman, *et al.*, Nanoemulsion-induced enzymatic crosslinking of tyramine-functionalized polymer droplets, *J. Mater. Chem. B*, 2017, 5(25), 4835–4844.
- 36 T. Ashida, S. Sakai and M. Taya, Competing two enzymatic reactions realizing one-step preparation of cell-enclosing duplex microcapsules, *Biotechnol. Prog.*, 2013, 29(6), 1528–1534.
- 37 W. H. Tan and S. Takeuchi, Monodisperse Alginate Hydrogel Microbeads for Cell Encapsulation, *Adv. Mater.*, 2007, 19(18), 2696–2701.

